Observation of anticorrelated modal noise in a quasi single-mode laser diode with a Michelson interferometer

Jean-Philippe Poizat, Philippe Grangier

HAL Id: hal-00558919

https://hal-iogs.archives-ouvertes.fr/hal-00558919

Submitted on 3 Apr 2012

Observation of anticorrelated modal noise in a quasi-single-mode laser diode with a Michelson interferometer

Jean-Philippe Poizat and Philippe Grangier

Institut d'Optique, B.P. 147, F91403 Orsay Cedex-France

The light emitted by a quasi-single-mode free-running laser diode is sent through a Michelson interferometer, and the intensity noise of the outgoing light is studied with respect to the path difference between the two arms of the interferometer. The level of this noise is determined by very strong anticorrelations between the main mode and the many very weak, but noisy, longitudinal side modes. The different interference patterns of these various modes can modify the noise compensation effect, leading to a large excess noise. Phase-noise effects also come into the picture, since a Michelson interferometer tuned around a nonzero path difference is a dispersive element capable of converting phase noise into intensity noise. The observed data is in good agreement with a phenomenological model that attributes phase noise and correlated intensity noises to all the modes. The parameters of this model can be inferred from the experimental data. © 1997 Optical Society of America [S0740-3224(97)03111-1]

PACS numbers: 42.55.Px, 42.50.Dv, 42.62.Fi

1. INTRODUCTION

Reduction of intensity noise of laser diodes below the standard quantum limit (SQL) (or shot noise) was achieved about a decade ago (Ref. 1 and 2 and references therein). Intensity noise levels below the SQL are now commonly observed. These results are based on the faithful conversion of a regular electron flux into a regular photon flux, owing to the high-quantum efficiency of semiconductor light emitters. However, the exact mechanisms explaining why some laser diodes allow subshot-noise operation, and others do not, are still under investigations. Our purpose in this paper is to present elements that could contribute to a better understanding of these mechanisms.

It was observed a long time ago that the low total intensity noise of quasi-single-mode laser diodes can be caused by strong anticorrelations between the main mode and the weak longitudinal side modes.[3–8] These studies were mainly to investigate power dropouts statistics and had no references to the SQL. In this paper we focus on the importance of the weakly multimode behavior for determining the quantum-noise properties of continuous-wave quasi-single-mode laser diodes.[9–12] Researchers have demonstrated[12] quantum anticorrelations between the intensity noises of different longitudinal modes, bringing the total intensity noise below the SQL, by sending the output light of a laser diode into a high-resolution spectrometer and analyzing the noise of the different modes by varying the position and the size of the output slit. According to the analysis presented by Marin *et al.*,[12] this effect is due to mode competition within an homogeneously broadened gain medium. This anticorrelated modal noise is an important issue when the relevant

noise properties are those of the main mode alone, as is the case in spectroscopy or in telecommunications (wavelength multiplexing). The reliability of optical communication depends both on the noise and on the spectral properties of the light emitters, which are usually laser diodes. As we show in this paper, these two properties are in fact strongly connected.

Here we employ an alternative method to demonstrate the existence of mode anticorrelations in a quasi-single-mode free-running laser diode by using a Michelson interferometer.[13] The principle of the experiment is that, depending on the path difference between the arms of the interferometer, the fringe patterns of the different modes are not necessarily superimposed. When they are not superimposed, the compensation between the noise of the different modes is imperfect, giving rise to a large excess noise. However, for periodic values of the path difference, all the fringe patterns come back in phase, and a low-intensity noise level is recovered.

We have developed a phenomenological model describing the rather complex situation of a quasi-single-mode laser with a multimode noise behavior in a Michelson interferometer. We have also considered the phase noise[14–16] of the different modes. This model is compared with the experimental results, and the agreement is very good.

We first present and discuss the experimental observations (Section 2). The phenomenological model is developed in Subsection 3.A, and its results are compared with the experimental ones in Subsection 3.B. We give in Appendix A the detailed quantum calculation of the phase-to-amplitude conversion for a single mode in a Michelson interferometer. A theoretical analysis of phase-ampli-
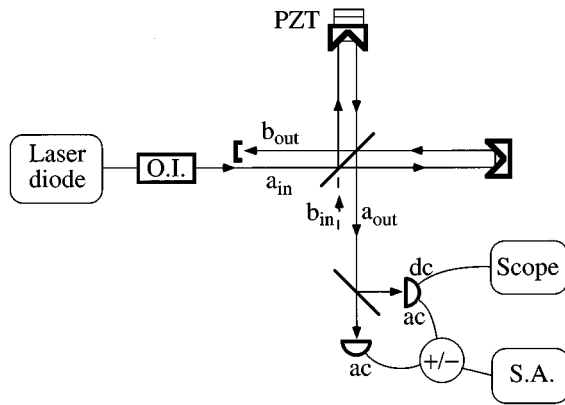
Fig. 1. Experimental setup. A 30-dB optical isolator avoids spurious feedback in the laser. The arm-length difference is controlled finely by a PZT and coarsely by a translation stage (not shown). The ac parts of the photocurrent are either added or substracted and sent to a spectrum analyzer (SA). The dc part of one of the detector is monitored on an oscilloscope together with the output signal of the SA.

tude correlations in a quasi-single-mode laser is sketched in Appendix B, and indications on the quantum multimode calculation are given in Appendix C.

2. EXPERIMENT

A. Experimental Setup
A sketch of the experimental setup is shown in Fig. 1. The laser diode is an index-guided quantum well GaAlAs device (model SDL 5411-G1) emitting at 800 nm, driven by a low-noise current source. The laser temperature is servo controlled. Its threshold current is $I_{\text{th}} = 18$ mA, and the operating current for the data presented in this paper is $I_{\text{op}} = 86$ mA. Using a spectrometer, we found that the measured free spectral range of the laser cavity is $\Delta\lambda = 0.11 \pm 0.05$ nm. The optical length of the cavity is therefore $L = \lambda^2/(2\Delta\lambda) = 2.9 \pm 0.15$ mm. We see below that this quantity is of interest in our experiment.

The noise detection is performed in the standard way, with a balanced configuration.[17] The SQL is recorded when the power combiner is switched to the minus position. The plus position gives the total-intensity noise. The detectors are large-area, high-efficiency pin photodiodes (EG&G C30809E). The laser light is attenuated by a factor of 4 to avoid saturation of the detectors. With this attenuation, the dc current is 2.4 mA for each detector. The ac currents are amplified with a low-noise amplifier and then combined and sent to an electronic spectrum analyzer. The noise is analyzed at a frequency of $\omega/(2\pi) = 10$ MHz with a 100-kHz bandwidth. The output of the spectrum analyzer is sent to an oscilloscope together with the dc signal of one of the detectors to allow simultaneous recording of the noise and the mean-field intensity.

The mirrors of the Michelson interferometer are corner cubes to prevent light from being reflected back into the laser. The contrast of the interferometer is better than 95%.

B. Experimental Results
For a set of different values of the arm-length difference l_a, the piezoelectric transducer (PZT) is slowly ($\sim$1 Hz) scanned over $\sim$2 fringes. Typical graphs are shown in Fig. 2.

For $l_a = 0$ [Fig. 2(a)] the fringe patterns of all the different modes are in phase (white fringe), so the noise compensation between the modes is as effective as it would be in the directly detected laser light. For vanishing armlength difference, phase-noise effects, which are proportional to $(\omega l_a/c)^2$, are also absent (cf. below and Appen-
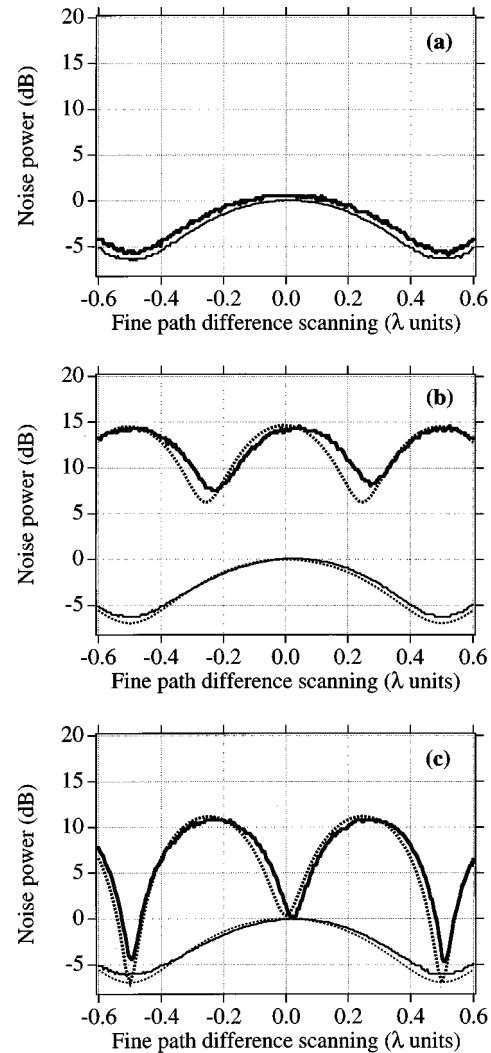

Fig. 2. Example of fine PZT scans for (a) $l_a = 0$, (b) $l_a = 1.44$ mm ($=0.47L$), and (c) $l_a = 3.06$ mm ($=L$). The solid curves are the experimental data, and the dashed curves are the theoretical fit. Note that for clarity there is no theoretical fit on graph (a). The upper traces are the output noise of the interferometer, and the lower traces are the SQL level (proportional to the light intensity). The 0-dB level corresponds to the SQL on a bright fringe. It is obvious by comparing the experimental and the theoretical SQL that the PZT scan is not rigorously linear. The SA resolution bandwidth is 100 kHz with a video filter of 30 Hz. Recall that the laser light is attenuated by a factor of 4. The fits are performed with five side modes on each side of the main mode ($M = 5$). The parameter used for the fits are $v_t = 1.1$, $v_p^{(0)} = 50$, $\gamma = 5$, $s = 0.3$, $v_q^{(0)} = 4.10^7$, and $v_q^{\text{sm}} = 4v_q^{(0)}$. The electronic noise level is 1/4 of the SQL at a bright fringe and is included in the fits.

dix A). Therefore the noise detected across the fringe scan is always the total-intensity noise of the laser, which is less than 1 dB above SQL.[12,15]

For $l_a = 0.475\,L$ [Fig. 2(b)] the fringe patterns of the different modes are somewhat randomly distributed. Some of the side modes are on a dark fringe, while the main mode is on a bright fringe or vice versa. The excess intensity noise of the main mode is then no longer compensated by the noise of the side modes, leading to a large-intensity noise at the output of the interferometer. The noise level at the top of a bright fringe is of the order of the intensity noise of the main mode alone. The noise minima on each side of a bright fringe can be simply understood if one assumes, for the sake of clarity, that all the anticorrelation is concentrated into one side mode. The noise is, therefore, equally split into the main mode and this side mode, but their noise fringe patterns are out of phase and therefore necessarily cross for some specific value of the path difference at the fine scanning level. At these specific locations the mode excess noise is, in principle, perfectly compensated (what remains is the phase noise, since now $(\omega l_a/c)^2 \neq 0$). These minima are to be found every $\lambda/4$, and their position relative to the main-mode fringe pattern depends on the dephasing between the two noise fringe patterns and therefore on the path difference at the coarse scanning level. In Fig. 2(b) the absolute noise level is the same at a dark fringe and at a bright fringe. This is because the excess noise at a bright fringe is due to the lack of compensation of the main-mode intensity noise by all the destructively interfering side modes. It is precisely this missing part that is found at a dark fringe, exhibiting thus the same absolute noise. Note that for $0 < l < L$ the phase-noise effects have a minor influence (see below and Appendix A).

For $l_a = L$ [Fig. 2(c)] the fringe patterns of all the modes are back in phase; the individual mode excess noise compensation is therefore maximum, as for $l_a = 0$. However, as can be seen in the figure, the noise pattern is different from the $l_a = 0$ case. This difference comes from the fact that the laser phase noise is now visible since $(\omega l_a/c)^2 \neq 0$. The interferometer is a dispersive device that acts as a quadrature rotator (cf. Appendix A) and projects the very large laser phase noise onto the amplitude quadrature outside of a bright fringe.[14] The maximum noise level reached on the flanks gives the total phase noise (main mode plus side modes). At the very top of a bright fringe the noise level is the laser intensity noise level.

We recorded 35 of these plots from $l_a = 0$ to $l_a = 2.4\,L$. We extracted four characteristic quantities from these plots and compiled them into the four graphs of Fig. 3. The first important observation on the graphs of Fig. 3 is that there is a periodic behavior with a periodicity equal to the laser cavity optical length $L = 3.05$ mm.[13] This is due to the presence of anticorrelations between modes.[9,12] Another important point is that we also have access to information about the phase noise of the different modes. In this experiment the specific use of a Michelson inter-
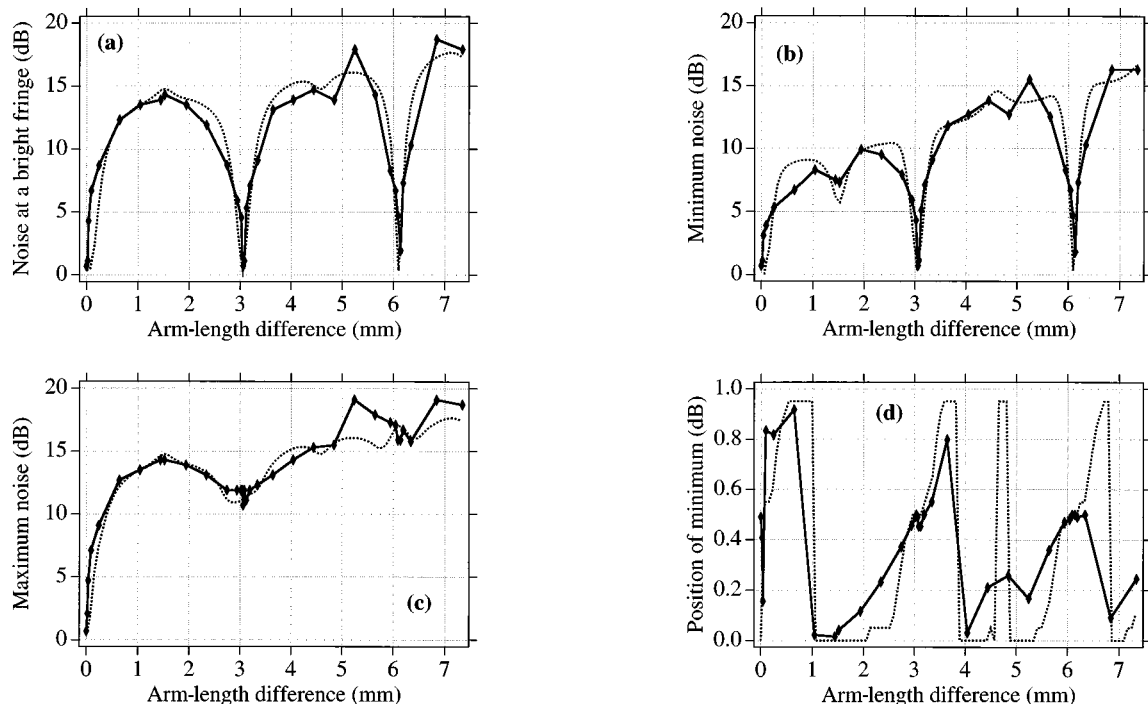

Fig. 3. These graphs compile four important quantities of fine PZT scans (cf. Fig. 2) for different values of the arm-length difference. The x axis is the interferometer arm-length difference l_a (in millimeters). The quantities displayed on the y axis are (a) the intensity noise at the top of a bright fringe, (b) the minimum and (c) the maximum noise level over a fine PZT scan, and (d) the position of the minimum relative to the fringe pattern (d). The minima considered in graphs (b) and (d) are the ones closest to a bright fringe. In graph (d) the minimum position is equal to 0.5 when the noise minimum is at the top of a bright fringe [like on Fig. 2(c)], and it is equal to 0 or 1 when the noise minimum is halfway between a dark and a bright fringe. For all these graphs the diamonds are the experimental data (the solid curve linking them is just a guide for the eye), and the dashed curves are the theoretical fits. Recall that the laser light is attenuated by a factor of 4. The parameters used for the fits are identical to the ones used in Fig. 2.

ferometer as a spectral discriminator allows mode anti-correlation and phase-noise effects[14,15] to appear simultaneously.

Before describing in more detail the four graphs of Fig. 3, we shall first discuss the relative size of the individual mode excess noise with respect to the phase noise. When $l_a = sL$ with s integer, the individual mode excess noises are compensated (to as low as 1 dB above the SQL), and only the phase-noise effects are present. Elsewhere, the order of magnitude of the noncompensated mode excess noises is the individual noise of the main mode $v_p^{(0)}$. With the notation introduced in detail in the Subsection 3.A, the order of magnitude of the phase noise of the main mode is $v_q^{(0)}(\omega l_a/c)^2$ (cf. Appendix A). So let us define a critical length $l_c = (c/\omega)(v_p^{(0)}/v_q^{(0)})^{1/2}$ at which the main-mode phase-noise effects become of magnitude equal to the main-mode intensity noise. Phase-noise effects come in when $l \geqslant l_c$. With the fitting parameters used in Figs. 2 and 3, we find $l_c = 5.3$ mm. This estimation was done without accounting for the side-mode phase noises, which introduces more phase noise in the system and leads to a slight lowering of the value of the critical length l_c, as can be seen on the experimental results.

The first relevant quantity out of the four graphs that we choose to display in Fig. 3 is the noise at the top of a bright fringe [Fig. 3(a)]. The height of the first arch gives the main-mode intensity noise. The fact that the height of the following arches slightly increases as the arm-length difference increases is attributed to the phase noise of the side modes. The phase noise of the main mode does not have an influence here since the noise is taken at the top of one of its own fringes, where there is no quadrature rotation.

The second quantity is the noise level at the noise minimum closest to the bright fringe [Fig. 3(b)]. It singles out information about the importance of the phase-noise effects, since the noise remaining at a minimum is mostly caused by phase noise (except when $l_a = sL$, where the noise minimum is at the top of a bright fringe and corresponds therefore only to intensity noise). The upperenvelope of the curves (i.e., without the points around $l_a = sL$) gives the level of the phase noise. For $l_a \approx l_c$ (critical length defined above) this envelope comes to the level of the intensity noise of the main mode alone.

The third quantity is the maximum noise level [Fig. 3(c)]. It is the upperenvelope of everything and therefore provides information about the noise level of the dominant noise source.

The fourth quantity is the position of the noise minima relative to the laser fringe pattern [Fig. 3(d)]. Note that, since the SQL is proportional to the intensity, the laser fringe pattern is analogous to the shot-noise fringe pattern. To fit these experimental results, we had to introduce an asymmetry in the noise of the different side modes. We did this in the model by shifting the origin of the even function attenuating the intensity noise of the side modes [see function $f(m)$ in Subsection 3.A]. This is physically justified since the frequency of the main mode usually does not coincide with the frequency of the maximum laser gain.

We performed this whole experiment for different laser temperatures (from 10 °C to 25 °C). Changing the laser temperature shifts spectrally the gain profile of the semiconductor, which has an influence on the multimode behavior of the laser and especially on its asymmetry. We did observe weak quantitative modifications in the noise behavior, which correspond to slightly different values of the main-mode intensity and the phase noises.

3. PHENOMENOLOGICAL MODEL

A. Model

In this model there is one noisy main mode [labeled (0)] that has a large mean photon number and $2M$ noisy longitudinal side modes with negligible mean photon number. The side modes thus do not contribute to the mean-field fringes, and their frequencies $\Omega^{(m)}$ for $m \in \{-M, -M+1, ..., M-1, M\}$ are given by

$$\Omega^{(m)} = \Omega_0 + m\mu, \qquad (1)$$

where μ is the free spectral range of the laser cavity, i.e., $\mu = c/(2L)$, where L is the optical length of the cavity.

The intensity noises of the side modes are independent and are anticorrelated with the intensity noise of the main mode [cf. Eqs. (B9) and (B10) of Appendix B]. Each mode has also a very large phase noise due to Schawlow–Townes phase diffusion.[18]

An important question is whether one should include in the model phase-amplitude correlations that could be induced by the so-called α parameter.[19] From an experimental point of view the effect of α would be to create an asymmetry in the noise power when a fringe is scanned; this effect has already been exploited to reduce the observed noise in a distributed feedback laser driven just above threshold.[20,21] In our case, when the laser is operated five times above threshold, no such asymmetry is observed. However, the absence of phase-amplitude correlations does not imply that $\alpha = 0$. It only means that far above threshold, the measured output-intensity noise is not coupled to the carrier fluctuations, which induce phase noise and linewidth broadening through the α parameter. Such a behavior was previously predicted for a single-mode laser operating far above threshold.[21] From our observations it can be deduced that the same behavior occurs in the quasi-single-mode case; a theoretical justification of this observation is sketched in Appendix B.

For simplicity the model is presented for $M = 1$ (one mode on each side of the main mode). All the information concerning the amplitude and the phase noises of the laser modes is contained in the $(4M + 2) \times (4M + 2)$ input symmetrized covariance matrix $\mathscr{S}_{\mathrm{in}}{}^a(\omega)$. The superscript a labels the input port of the Michelson interferometer (cf. Fig. 1). Using symmetrized products, we define this matrix by

$$\mathscr{S}_{\mathrm{in}}{}^a(\omega) = \delta\mathbf{p}_{\mathrm{in}}(\omega)[\delta\mathbf{p}_{\mathrm{in}}(-\omega)]^T, \qquad (2)$$

where, for M=1,

$$\mathbf{p}_{\mathrm{in}}(\omega) = [\, p_{\mathrm{in}}^{(-1)}(\omega),\ q_{\mathrm{in}}^{(-1)}(\omega),\ p_{\mathrm{in}}^{(0)}(\omega),\ q_{\mathrm{in}}^{(0)}(\omega),$$

$$p_{\mathrm{in}}^{(1)}(\omega),\ q_{\mathrm{in}}^{(1)}(\omega)\,]^T, \qquad (3)$$

with $p_{\mathrm{in}}^{(m)}$ ($q_{\mathrm{in}}^{(m)}$) being the amplitude (phase) of mode m, and $\delta p = p - \langle p \rangle$. The output symmetrized covariance matrix is defined similarly by $\mathscr{S}_{\mathrm{out}}{}^a(\omega) = \delta\mathbf{p}_{\mathrm{out}}(\omega)$

$\times [\delta\mathbf{p}_{\text{out}}(-\omega)]^T$. Note that all the noises are in units of the main mode SQL. The SQL of a side mode is proportional to its intensity, which has been neglected in this model. The noises of the side modes are thus very large compared with their own SQL and are therefore treated as classical noises. This means that the $(4M + 2)$ $\times (4M + 2)$ symmetrized covariance matrix $\mathscr{S}^b(\omega)$ of the vacuum state corresponding to the other input of the interferometer (cf. Fig. 1) has no vacuum noise contribution for the side modes and is taken to be equal to

$$\mathscr{S}_{\text{in}}{}^b(\omega) = \begin{bmatrix} O & O & O \\ O & \begin{pmatrix} 1 & 0 \\ 0 & 1 \end{pmatrix} & O \\ O & O & O \end{bmatrix}. \tag{4}$$

In our model there are intermode correlations only between the amplitudes, and, as already said, the phase of a mode is coupled neither to its own amplitude nor to the total amplitude (Appendix B). Then arbitrary parameters (for an analysis frequency $\omega/2\pi = 10$ MHz) are the following:

• The total intensity noise v_t (normalized to the SQL) of the laser diode with a direct detection. This quantity is given by the noise level for $l_a = 0$ [Fig. 2(a)].

• The main-mode intensity noise $v_p^{(0)} = \langle \delta p^{(0)}(\omega)\delta p^{(0)}(-\omega)\rangle$ (normalized to the SQL). Its value is directly inferred from the height of the first arch in Fig. 3(a).

• The die-away function $f(m)$ gives the relative contribution of side mode m. This function is chosen equal to $f(m) = 10^{-(m+s)/\gamma}$, where γ is the die-away coefficient, and s describes an eventual asymmetry in the intensity noise of the side modes. The γ coefficient is adjusted to fit the general shape of the archs of Fig. 3(a), whereas s is deduced from the relative position of the fringe minimum [Fig. 3(d)]. The exact expression for the intensity noise of mode m is given below [Eq. (5)].

• The phase-noise level of the main mode $v_q^{(0)}$ $= \langle \delta q^{(0)}(\omega)\delta q^{(0)}(-\omega)\rangle$ (normalized to the SQL). The value of the total (i.e., main mode plus side modes) phase noise is given by the maximum noise level in a fine scan for $l_a = L$ [Fig. 2(c)]. The side-mode phase noise can be obtained independently (see below and Subsection 3.B).

• The side-mode phase-noise level is $v_q{}^{\text{sm}}$ (normalized to the main mode SQL). Its value is deduced from the arch height increase in Fig. 3(a) and the position of the fringe minimum [Fig. 3(d)]. The exact phase noise of mode m is given in Eq. (6).

Without any loss of generality, all the uncorrelated intensity noise v_t is concentrated into the main mode. The intensity noise of mode m is given by

$$\langle \delta p^{(m)}(\omega)\delta p^{(m)}(-\omega)\rangle = (v_p^{(0)} - v_t)[f(m)]^2/N, \tag{5}$$

where $N = \Sigma_{m\neq 0}[f(m)]^2$ is a normalization coefficient. The total intensity noise v_t appears then as the result of an imbalance between the main-mode and the side-mode noises.[12]

The phase noise of mode m ($m \neq 0$) is given by

$$\langle \delta q^{(m)}(\omega)\delta q^{(m)}(-\omega)\rangle = v_q{}^{\text{sm}}(\omega)[f(m)]^2/N. \tag{6}$$

The only nonzero intensity correlations are those between each side mode and the main mode (Appendix B). They are given by

$$\langle \delta p^{(m)}(\omega)\delta p^{(0)}(-\omega)\rangle = \langle \delta p^{(0)}(\omega)\delta p^{(m)}(-\omega)\rangle$$
$$= -v_p^{(m)}(\omega). \tag{7}$$

The quadrature rotation matrices $\mathscr{R}^a(\omega)$ and $\mathscr{R}^b(\omega)$, which describe how the phase noise is converted into the intensity noise for the laser and for the vacuum, respectively, are built by blocks from the matrices $R^a(\omega)$ and $R^b(\omega)$ given in Eqs. (A9) and (A10) of Appendix A. We have

$$\mathscr{R}^a(\omega) = \begin{bmatrix} R_{(-1)}^a(\omega) & O & O \\ O & R_{(0)}^a(\omega) & O \\ O & O & R_{(1)}^a(\omega) \end{bmatrix} \tag{8}$$

and a similar equation for $\mathscr{R}^b(\omega)$.

The symmetrized output noise covariance matrix is given by

$$\mathscr{S}_{\text{out}}(\omega) = \delta\mathbf{p}_{\text{out}}(\omega)[\delta\mathbf{p}_{\text{out}}(-\omega)]^T$$
$$= \mathscr{R}^a(\omega)\mathscr{S}_{\text{in}}{}^a(\omega)[\mathscr{R}^a(-\omega)]^T + \mathscr{R}^b(\omega)\mathscr{S}_{\text{in}}{}^b(\omega)$$
$$\times [\mathscr{R}^b(-\omega)]^T. \tag{9}$$

Note that this equation is formally identical to Eq. (A11) of Appendix A.

The absolute noise of mode m is the product of its fluctuations $\delta p^{(m)}(\omega)$ by $\sin(\Omega^{(m)}l_a/c)$. A rigorous explanation of this can be given in the framework of the fully quantum multimode calculation, where the absolute noise of each mode is obtained by multiplication of its SQL-normalized fluctuations by the field of its local oscillator (Appendix C). The absolute amplitude noise $\delta P_{\text{out}}^{(m)}(\omega)$ of mode m is given by

$$\delta P_{\text{out}}^{(m)}(\omega) = \delta p^{(m)}(\omega)\sin(\Omega^{(m)}l_a/c). \tag{10}$$

The total-intensity noise $B_{\text{out}}(\omega)$ is thus given by

$$B_{\text{out}}(\omega) = \left[\sum_{m=-M}^{M} \delta P_{\text{out}}^{(m)}(\omega)\right]\left[\sum_{m=-M}^{M} \delta P_{\text{out}}^{(m)}(-\omega)\right]. \tag{11}$$

B. Comparison with the Experiment

The fits between the phenomenological model and the experimental results are performed with the six arbitrary parameters introduced above. Among them, the total-intensity noise level v_t, the main-mode intensity noise $v_p^{(0)}$, the main-mode phase noise $v_q^{(0)}$, and the side-mode phase noise v_q^{sm} have a clear physical meaning. Their values can be inferred almost independently from the various figures as mentioned above (Subsection 3.A). This facilitates the optimization procedure of the multiparameter fit. The physical contents of the die-away function $f(m)$ (two parameters) is, however, less straightforward. The calculation has been done with five side modes on each side of the main mode ($M = 5$), while the

real laser has more than 150 on each side.[12] The die-away coefficient γ is therefore more of an ad hoc parameter introduced to describe the 150 side modes with only five. Finally, the main influence of the values of the asymmetry parameter s is on the position of the noise minimum in Fig. 3(d).

Note that the same set of parameters has been used for all the graphs of Figs. 2 and 3. The agreement between theory and experiment is globally quite satisfactory. It allows us to extract the useful information.

The total-intensity noise v_t is obtained directly from Fig. 2(a) with an accuracy of 0.2 dB. Its value is v_t = 1.1 ± 0.04 (a value of 1 would correspond to the SQL). The excess intensity noise of the main mode $v_p^{(0)}$ is independently deduced from the fit (±1 dB) to the first arch of Fig. 3(a). Its value is $v_p^{(0)} = 50 \pm 10$. These two quantities are completely independent and are obtained from a one-parameter fit. The uncertainties are directly inferred from the experimental accuracy as can be seen on the corresponding graphs. The total amount of phase noise $v_q^{(0)} + v_q^{\mathrm{sm}}$ [including all side modes; Eq. (6)] can also be evaluated in a single-parameter fit from Fig. 2(c) to better than 1 dB. The magnitude of the side-mode phase noise is determined by the global slope in Fig. 3(c), but the relative weight of the two contributions has, however, a rather large uncertainty (±3 dB). The best fits are obtained for $v_q^{(0)} = 4.10^7$ and $v_q^{\mathrm{sm}} = 4v_q^{(0)}$. The asymmetry parameter s is estimated from the general shape of Fig. 3(d), and its value is $s = 0.2 \pm 0.1$. Note that the fine scan curves in the second arch ($L < l_a < 2L$) are almost flat, which renders the position of the minima not very meaningful, and therefore the discrepancy in the fit not very important. The die-away coefficient γ is taken to match the general shape of the archs in Fig. 3(a), given the limited number of modes ($M = 5$) used in the model.

Also recall that these plots have been obtained with an attenuation of the laser beam by a factor of 4 (6 dB), and that for convenience the fits have been performed on this raw data. An extra 1 dB, when the propagation losses and the detection efficiency are considered, has also to be added to obtain the true noises at the laser output. The real total-intensity noise is then 1.8 ± 0.2 dB above the SQL like in our previous measurements[12,15] where it was 2 dB. The true phase noise is 83 ± 2 dB above the SQL, which agrees with the value (82 ± 1 dB) found for the same laser with another setup with an 8-MHz bandwidth (HWHM) Fabry–Perot cavity.[15] The main-mode intensity noise is found to be 24 ± 1 dB above the SQL, while the value found with a high-resolution spectrometer for another similar laser from the same manufacturer was 39 ± 1 dB.[12]

This last quantitative change can be attributed to the fact that the multimode noise characteristic of a laser diode is very sensitive to laser temperature, extremely weak feedback in the laser, etc. It is therefore very difficult to recover exactly identical experimental conditions from one experimental setup to another. Nevertheless, the qualitative behavior of the system is very well described by our model and confirms the main results of Refs. 12 and 15, which are respectively the existence of very strong anticorrelations between main-mode and side-mode intensity noises, and very large phase noise.

Note that we have also tried to fit the experimental data with a model in which the side modes are individually correlated with each other. The best fit was not as good as the one presented in Fig. 3, which was obtained with uncorrelated side modes. The assumption used in the paper is therefore clearly constrained by the data. Moreover, it is supported by theoretical evidence (Appendix B).

4. CONCLUSION

In this paper we have used an alternative method employing a Michelson interferometer to demonstrate and confirm that the low level of intensity noise of some quasi-single-mode laser diodes is caused by strong anticorrelations between the main mode on the one hand and a large number of longitudinal side modes on the other hand.[12]

Furthermore, a correct description of this system requires the inclusion of phase-noise effects. It has been shown[15] that free-running laser diodes have extremely large phase noise (more than 80 dB above the SQL). A Michelson interferometer is a dispersive device that converts phase noise into intensity noise, therefore bringing phase noise into the picture. However, phase-amplitude coupling effects within the laser[19] did not show up in the experimental results and have therefore not been included in the theory. This behavior is in agreement with the theoretical predictions from a model published earlier.[12]

The phenomenological model we have developed includes phase noise as well as correlations of the longitudinal modes intensity noise. This model fits quite well with the experimental results and allows the quantitative determination of useful parameters such as the individual intensity noise of the main mode and its phase noise. These values are in reasonably good agreement with previously published results.[12,15]

APPENDIX A: QUADRATURE ROTATION AFTER PROPAGATION IN A MICHELSON INTERFEROMETER

In this appendix we derive the rotation undergone by the quadrature components of a single-mode light beam with an optical frequency $\Omega/2\pi$ at an analysis frequency $\omega/2\pi$ after propagation through a Michelson interferometer. Using the definitions of the field operators given in Fig. 1, we obtain the input–output relation for the field operators:

$$u_{\mathrm{out}}(\omega) = A(\omega)u_{\mathrm{in}}(\omega) + B(\omega)v_{\mathrm{in}}(\omega), \qquad (A1)$$

with

$$u_{\mathrm{in,out}}(\omega) = \begin{bmatrix} a_{\mathrm{in,out}}(\omega) \\ a_{\mathrm{in,out}}^{\dagger}(\omega) \end{bmatrix}, \quad v_{\mathrm{in,out}}(\omega) = \begin{bmatrix} b_{\mathrm{in,out}}(\omega) \\ b_{\mathrm{in,out}}^{\dagger}(\omega) \end{bmatrix},$$
$$(A2)$$

$$A(\omega) = \begin{bmatrix} -i\,\sin(s)\exp(is) & 0 \\ 0 & i\,\sin(d)\exp(-id) \end{bmatrix},$$
(A3)

$$B(\omega) = \begin{bmatrix} \cos(s)\exp(is) & 0 \\ 0 & \cos(d)\exp(-id) \end{bmatrix},$$
(A4)

where $s = (\Omega + \omega)l_a/c$, $d = (\Omega - \omega)l_a/c$, and l_a is the length difference between the two arms of the interferometer (the optical path difference is equal to $2l_a$). The input laser light is described by $a_{in}(\omega)$, and $b_{in}(\omega)$ accounts for the vacuum field entering the unused port of the interferometer. Note that we have $a_{in}^\dagger(\omega) = [a_{in}(-\omega)]^\dagger$ and a similar equation for the other operators.

The amplitude and the phase quadratures are defined by

$$U_{in,out} = T_{in,out}u_{in,out},$$

$$V_{in,out} = T_{in,out}v_{in,out},$$
(A5)

with

$$U_{in,out} = \begin{bmatrix} p_{in,out}{}^a(\omega) \\ q_{in,out}{}^a(\omega) \end{bmatrix}, \qquad V_{in,out} = \begin{bmatrix} p_{in,out}{}^b(\omega) \\ q_{in,out}{}^b(\omega) \end{bmatrix},$$
(A6)

$$T_{in} = \frac{1}{\sqrt{2}}\begin{bmatrix} 1 & 1 \\ -i & i \end{bmatrix},$$

$$T_{out} = \frac{1}{\sqrt{2}}\begin{bmatrix} i\,\exp(-i\Omega l_a/c) & -i\,\exp(i\Omega l_a/c) \\ \exp(-i\Omega l_a/c) & \exp(i\Omega l_a/c) \end{bmatrix}. \quad (A7)$$

So if we turn into the quadrature basis, we obtain

$$U_{out}(\omega) = T_{out}A(\omega)T_{in}{}^{-1}U_{in}(\omega) + T_{out}B(\omega)T_{in}{}^{-1}V_{in}(\omega),$$
(A8)

where $T_{out}A(\omega)T_{in}{}^{-1} = R^a(\omega)$ is explicitly given by

$$R^a(\omega) = \exp(i\omega l_a/c)\begin{bmatrix} \sin(\Omega l_a/c)\cos(\omega l_a/c) & i\,\cos(\Omega l_a/c)\sin(\omega l_a/c) \\ -i\,\cos(\Omega l_a/c)\sin(\omega l_a/c) & \sin(\Omega l_a/c)\cos(\omega l_a/c) \end{bmatrix}, \quad (A9)$$

and $T_{out}B(\omega)T_{in}{}^{-1} = R^b(\omega)$ by

$$R^b(\omega) = \exp(i\omega l_a/c)\begin{bmatrix} -i\,\sin(\Omega l_a/c)\sin(\omega l_a/c) & -\cos(\Omega l_a/c)\cos(\omega l_a/c) \\ \cos(\Omega l_a/c)\cos(\omega l_a/c) & -i\,\sin(\Omega l_a/c)\sin(\omega l_a/c) \end{bmatrix}. \quad (A10)$$

If the two fields a and b have independent fluctuations, the symmetrized noise covariance matrix S_{out} of the output beam a_{out} is then given by

$$S_{out}(\omega) = \delta U_{out}(\omega)[\delta U_{out}(-\omega)]^T$$
$$= R^a(\omega)S_{in}{}^a(\omega)[R^a(-\omega)]^T$$
$$+ R^b(\omega)S_{in}{}^b(\omega)[R^b(-\omega)]^T, \quad (A11)$$

where the symmetrized input covariance matrices are

$$S_{in}{}^a(\omega) = \langle \delta U_{in}(\omega)[\delta U_{in}(-\omega)]^T\rangle,$$

$$S_{in}{}^b(\omega) = \langle \delta V_{in}(\omega)[\delta V_{in}(-\omega)]^T\rangle. \quad (A12)$$

Note that $S_{in}{}^a(\omega)(1, 1)$ and $S_{in}{}^a(\omega)(2, 2)$ are, respectively, the amplitude and the phase noise of the input laser light. The off-diagonal terms account for the amplitude–phase correlations. For a standard vacuum, we have $S_{in}{}^b(\omega) = \mathbf{I}$.

The SQL is proportional to the intensity at the output port. Assuming that the b field is the vacuum, the SQL is proportional to $\sin^2(\Omega l_a/c)$. The absolute noise fluctuations are given by the product of the SQL-normalized noise fluctuations $\delta U_{out}(\omega)$ by the field of the local oscillator that is the mean field $p_{out}{}^a\,\sin(\Omega l_a/c)$. The absolute noise power $N_{out}(\omega)$ is then given by (see Appendix C)

$$N_{out}(\omega) = S_{out}(\omega)\sin^2(\Omega l_a/c). \quad (A13)$$

APPENDIX B: PHASE−AMPLITUDE COUPLING IN QUASI-SINGLE-MODE LASER DIODES

The purpose of the calculation presented here is to point out that a nonzero value of the well-known α or Henry's parameter,[19] which couples the phase noise to the carrier fluctuations, does not imply the existence of correlations between the output intensity and the phase noise of the laser. This is true even if α contributes significantly to increase the laser linewidth, and it is basically because, far above threshold, the output intensity noise is decoupled from the noise sources that contribute to the laser phase and/or frequency noise. It was already demonstrated by Karlsson and Björk[21] that, in a single-mode laser driven far above threshold, there are no correlations between the intensity and the phase noise of the output beam. We show in this appendix that the situation is similar for a homogeneously broadened multimode laser diode driven far above threshold.

The quasi-single-mode laser diode is described by three modes (one main mode, labeled 0 and two side modes, labeled -1 and 1) coupled to a common carrier population (homogeneous behavior).[9,12] The dynamic variables are the internal electromagnetic fields $a^{(m)}$ of the mode (m), and the total number of excited carriers N. Rather than using the field variables, we use the photon numbers $n^{(m)}$ and the phase fluctuations $\delta\phi^{(m)}$. The latter is defined in the linearized approximation as $[\langle a^{(m)\dagger}\rangle\delta a^{(m)}$

$- \langle a^{(m)} \rangle \delta a^{(m)\dagger}]/[2i\langle n^{(m)} \rangle]$.   The equations obeyed by the photon numbers are then

$$\frac{dn^{(m)}(t)}{dt} = -\frac{n^{(m)}}{\tau^{(m)}} + N(t)A^{(m)}(n^{(m)}(t) + 1) + f_r^{(m)}(t)$$

$$+ G_r^{(m)}(t) \qquad (B1)$$

and can be linearized around the steady-state values to yield

$$\frac{d\delta n^m(t)}{dt} = \frac{1}{2}\left(-\frac{1}{\tau^{(m)}} + \langle N \rangle A^{(m)}\right)\delta n^{(m)}(t)$$

$$+ \langle n^{(m)} + 1 \rangle A^{(m)} \delta N(t) + f_r^{(m)} + G_r^{(m)}. \qquad (B2)$$

We will not write the imaginary part of the field equations, which determines the frequencies of the modes, but directly give the linearized equations for the phase noise in each mode:

$$\frac{d\delta\phi^{(m)}(t)}{dt} = \alpha^{(m)}A^{(m)}\delta N(t) + \frac{1}{\langle n^{(m)} \rangle}[f_i^{(m)}(t)$$

$$+ G_i^{(m)}(t)]. \qquad (B3)$$

In the equations above, the quantity $1/\tau^{(m)}$ is the photon decay rate of mode (m), which we assume to be present only because of the output coupling mirror. (The role of optical losses will be discussed below.) The coefficient $A^{(m)}$ is the spontaneous emission rate into the corresponding lasing mode. The $\alpha^{(m)}$ parameter is the phase-carrier coupling coefficient.[19] The last terms are Langevin noise terms, with real (r) and imaginary (i) parts defined with respect to the average fields $\langle a^{(m)} \rangle$. These noises are respectively associated with the stimulated-emission gain [correlation $\langle G_i^{(m)}(t)G_i^{(m)}(t') \rangle = \langle G_r^{(m)}(t)G_r^{(m)}(t') \rangle = \delta(t - t')A^{(m)}\langle N \rangle\langle n^{(m)} \rangle$] and the output coupling [correlation $\langle f_i^{(m)}(t)f_i^{(m)}(t') \rangle = \langle f_r^{(m)}(t)f_r^{(m)}(t') \rangle = \delta(t - t')\langle n^{(m)} \rangle/\tau^{(m)}$].

The equation of motion for the total excited carrier number $N(t)$ is

$$\frac{dN(t)}{dt} = P - \frac{N(t)}{\tau_{sp}} - \sum_m A^{(m)}(n^{(m)}(t) + 1)N(t)$$

$$+ \Gamma_{(p)}(t) + \Gamma_{(sp)}(t) + \Gamma_{(st)}(t), \qquad (B4)$$

where P is the pumping rate and τ_{sp} is the spontaneous electron lifetime. The last three terms are Langevin noises. The first one, $\Gamma_{(p)}(t)$, is associated with the pump noise, and for a pump-noise-suppressed laser its correlation function is $\langle \Gamma_{(p)}(t)\Gamma_{(p)}(t') \rangle = 0$. The terms $\Gamma_{(sp)}(t)$ and $\Gamma_{(st)}(t)$, associated with spontaneous and stimulated emission noise, respectively, have correlations $\langle \Gamma_{(sp)}(t)\Gamma_{(sp)}(t') \rangle = \delta(t - t')\langle N \rangle/\tau_{sp}$ and $\langle \Gamma_{(st)}(t)\Gamma_{(st)}(t') \rangle = \delta(t - t')\Sigma_m A^{(m)}\langle N \rangle\langle n^{(m)} \rangle$. Finally, owing to their same physical origin, the noise terms associated with the stimulated gain for the photons and the stimulated emis-

sion for the electrons are perfectly anticorrelated and have cross correlations $\langle G_r^{(m)}(t)\Gamma_{(st)}(t') \rangle = -\delta(t - t')A^{(m)}\langle N \rangle\langle n^{(m)} \rangle$.

In our situation the laser is operating in quasi-single mode far above threshold. Therefore the numbers of photons in the side modes $n^{(-1, 1)}(t)$ are small and are taken as first-order corrections, and one has $n^{(0)} + 1 \approx n^{(0)}$. Defining $P_{th} = 1/(A^{(0)}\tau^{(0)}\tau_{sp})$ and $p^{(-1, 1)} = (A^{(-1, 1)}\tau^{(-1, 1)})/(A^{(0)}\tau^{(0)})$, the stationary solutions far above threshold are $\langle N \rangle = P_{th}\tau_{sp}$, $\langle n^{(0)} \rangle = (P - P_{th})\tau^{(0)}$, and $\langle n^{(-1, 1)} \rangle = p^{(-1, 1)}/(1 - p^{(-1, 1)})$. The linearized equations around these stationary values are then Fourier transformed, and one obtains for the fluctuations at zero frequency

$$A^{(0)}\langle n^{(0)} \rangle \delta N = -(f_r^{(0)} + G_r^{(0)}), \quad (B5)$$

$$(1 - p^{(-1, 1)})\delta n^{(-1, 1)}/(2\tau^{(-1, 1)}) = A^{(-1, 1)}\langle n^{(-1, 1)} \rangle \delta N$$

$$+ f_r^{(-1, 1)} + G_r^{(-1, 1)}, \qquad (B6)$$

$$A^{(0)}\langle N \rangle \delta n^{(0)} = -(1/\tau_{sp} + A^{(0)}\langle n^{(0)} \rangle)\delta N$$

$$- \langle N \rangle(A^{(-1)}\delta n^{(-1)}$$

$$+ A^{(1)}\delta n^{(1)})$$

$$+ \Gamma_{(p)} + \Gamma_{(sp)} + \Gamma_{(st)}. \qquad (B7)$$

The output intensity noise can be obtained by use of the standard input–output relation:

$$\delta n_{out}^{(m)} = (1/\tau^{(m)})\delta n^{(m)} - f_r^{(m)}. \qquad (B8)$$

To obtain a simple expression for the output photon number fluctuations, we use the input–output relation [Eq. (B8)], neglect noise terms whose correlations or autocorrelations are proportional to $\langle n^{(-1, 1)} \rangle$, and neglect the terms $\delta N/\tau_{sp}$ and $\Gamma_{(sp)}$ because of far-above-threshold operation. From Eqs. (B5)–(B8) one then obtains

$$\delta n_{out}^{(0)} = -(\delta n_{out}^{(-1)} + \delta n_{out}^{(1)}) + \Gamma_{(p)}, \qquad (B9)$$

$$\delta n_{out}^{(-1, 1)} = 2\langle n^{(-1, 1)} \rangle(f_r^{(-1, 1)} + G_r^{(-1, 1)}). \qquad (B10)$$

It can be seen from these equations that the total intensity noise $\Sigma \delta n_{out}^{(m)}$ is only limited by the pump noise, exactly like δn_{out} in a single-mode laser. On the other hand, $\delta n_{out}^{(-1)}$ ($\delta n_{out}^{(1)}$) depends only on the Langevin forces with subscript (-1) [(1)]. The side-mode fluctuations are therefore uncorrelated with each other. Finally, when the expression of δN given by Eq. (B5) is used, Eq. (B3) becomes

$$\frac{d\delta\phi^{(m)}(t)}{dt} = \frac{-\alpha^{(m)}}{\langle n^{(1)} \rangle}(f_r^{(0)} + G_r^{(0)})$$
$$+ \frac{1}{\langle n^{(m)} \rangle}(f_i^{(m)} + G_i^{(m)}). \qquad (B11)$$

It can be straightforwardly deduced from Eq. (B11) that the laser linewidth of the main mode will be increased by the usual factor $(1 + \alpha^2)$ with respect to the Schawlow–Townes linewidth,[18] where the noise associated with α^2 comes from the real part of the Langevin noise.

Looking at the total-intensity noise at the laser output, it is clear that the term owing to the carrier number fluctuations is compensated by the $f_r^{(0)}$ and $G_r^{(0)}$ terms in the Langevin noise term far above threshold: this is the origin of squeezing effect, which remains limited by the term owing to the pump noise $\Gamma_{(p)}$. Therefore the total-intensity noise does not depend anymore on the Langevin noise in the main mode, in contrast to the phase noise as shown by Eq. (B11) above. This behavior is the same as the one for a single-mode diode, considered by Karlsson and Björk[21]: the amplitude-phase correlations, which are present slightly above threshold, vanish with increasing pumping current. In this case one may ask whether the very large excess noise present in the individual modes will appear on the phase; the equations above show that this is not the case: as shown in Eq. (B11), the phase noise in mode (m) depends on the real part of the Langevin noise of the main mode (through the α parameter) and on the imaginary part of the Langevin noise of mode (m). None of these noise sources is coupled to the real part of the Langevin noise of the side modes, which determines the large intensity noise in the individual modes [Eq. (B10)].

From all the above remarks one can conclude that, in a quasi-single-mode laser driven far above threshold, the part of the laser phase noise owing to the carrier number fluctuations is correlated neither to the individual intensity noise nor to the total-intensity noise. This result is in agreement with our experimental observations. However, we point out that, in practice, the squeezing in the total-intensity noise is limited by other effects, which have been deliberately omitted so far: first, the optical losses inside the cavity, and second, the fact that the perfect anticorrelation between the modes is partially destroyed by various mechanisms, such as self-saturation of each mode[12] or nonlinear gain.[22] When these effects are considered, the calculation shows that the carrier noise picks up some contribution of the large excess noise of the individual modes. However, this contribution remains small in the range of parameters considered in Ref. 12, which is also relevant for this experiment.

APPENDIX C: HINTS ON THE MULTIMODE QUANTUM CALCULATION

In this appendix we briefly sketch a full multimode quantum calculation. Within this framework the mean values of the side-mode fields (written as $\epsilon^{(m)}$) are not neglected, and the noise of the side modes are normalized to their own SQL (denoted with a $_{\mathrm{SN}}$ subscript).

To get the absolute noise of mode m, the (SQL-normalized) fluctuations $\delta p_{\mathrm{SN}}^{(m)}(\omega)$ and $\delta q_{\mathrm{SN}}^{(m)}(\omega)$, which are respectively given by $\delta p^{(m)}(\omega)/\epsilon^{(m)}$ and $\delta q^{(m)}(\omega)/\epsilon^{(m)}$, have to be multiplied by the field of their local oscillator, which is nothing more than their own field $\epsilon^{(m)} \sin(\Omega^{(m)} l_a/c)$. Let us define an absolute fluctuation vector $\delta \mathbf{P}_{\mathrm{out}}(\omega)$ as (for $M = 1$)

$$\delta\mathbf{P}_{\mathrm{out}}(\omega)$$

$$= \begin{bmatrix} \delta P_{\mathrm{out}}^{(-1)}(\omega) \\ \delta Q_{\mathrm{out}}^{(-1)}(\omega) \\ \delta P_{\mathrm{out}}^{(0)}(\omega) \\ \delta Q_{\mathrm{out}}^{(0)}(\omega) \\ \delta P_{\mathrm{out}}^{(1)}(\omega) \\ \delta Q_{\mathrm{out}}^{(1)}(\omega) \end{bmatrix} = \begin{bmatrix} \epsilon^{(1)} \sin(\Omega^{(-1)} l_a/c)\,\delta p_{\mathrm{SN}}^{(-1)}(\omega) \\ \epsilon^{(1)} \sin(\Omega^{(-1)} l_a/c)\,\delta q_{\mathrm{SN}}^{(-1)}(\omega) \\ \epsilon^{(0)} \sin(\Omega^{(0)} l_a/c)\,\delta p_{\mathrm{SN}}^{(0)}(\omega) \\ \epsilon^{(0)} \sin(\Omega^{(0)} l_a/c)\,\delta q_{\mathrm{SN}}^{(0)}(\omega) \\ \epsilon^{(1)} \sin(\Omega^{(1)} l_a/c)\,\delta p_{\mathrm{SN}}^{(1)}(\omega) \\ \epsilon^{(1)} \sin(\Omega^{(1)} l_a/c)\,\delta q_{\mathrm{SN}}^{(1)}(\omega) \end{bmatrix}$$

$$= \begin{bmatrix} \sin(\Omega^{(-1)} l_a/c)\,\delta p^{(-1)}(\omega) \\ \sin(\Omega^{(-1)} l_a/c)\,\delta q^{(-1)}(\omega) \\ \sin(\Omega^{(0)} l_a/c)\,\delta p^{(0)}(\omega) \\ \sin(\Omega^{(0)} l_a/c)\,\delta q^{(0)}(\omega) \\ \sin(\Omega^{(1)} l_a/c)\,\delta p^{(1)}(\omega) \\ \sin(\Omega^{(1)} l_a/c)\,\delta q^{(1)}(\omega) \end{bmatrix}. \qquad (C1)$$

The result used in the main text is thus demonstrated.

So we can now define an absolute noise correlation matrix $\mathcal{N}_{\mathrm{out}}(\omega)$ by

$$\mathcal{N}_{\mathrm{out}}(\omega) = \delta\mathbf{P}_{\mathrm{out}}(\omega)[\mathbf{P}_{\mathrm{out}}(-\omega)]^T. \qquad (C2)$$

The total intensity noise at the output of the interferometer is given by

$$B_{\mathrm{out}}(\omega) = \left[\sum_{m=-M}^{M} \delta P^{(m)}(\omega) \right]\left[\sum_{m=-M}^{M} \delta P^{(m)}(-\omega) \right]. \qquad (C3)$$

The terms of this sum are to be picked up in the absolute noise-correlation matrix $\mathcal{N}_{\mathrm{out}}(\omega)$.

REFERENCES

1. S. Machida, Y. Yamamoto, and Y. Itaya, "Observation of amplitude squeezing in a constant-current-driven semiconductor laser," Phys. Rev. Lett. **58**, 1000 (1987).
2. W. H. Richardson, S. Machida, and Y. Yamamoto, "Squeezed photon-number noise and sub-Poissonian electrical partition noise in a semiconductor laser," Phys. Rev. Lett. **66**, 2867 (1991).
3. A. W. Smith and J. A. Armstrong, "Intensity noise in multimode GaAs laser emission," IBM J. Res. Dev. **10**, 225 (1966).
4. G. Arnold and K. Petermann, "Intrinsic noise of semiconductor laser in optical systems," Opt. Quantum Electron. **12**, 207 (1980).
5. C. H. Henry, P. S. Henry, and M. Lax, "Mode power partition events in nearly single-frequency lasers," J. Lightwave Technol. **LT-2**, 209 (1984).

6. R. A. Linke, B. L. Kasper, C. A. Burrus, I. P. Kaminow, J. S. Ko, and T. P. Lee, "Mode power partition events in nearly single-frequency lasers," J. Lightwave Technol. **LT-3**, 706 (1985).

7. G. L. Abbas and T. K. Yee, "Power dropout statistics of nearly-single-longitudinal mode semiconductor lasers," IEEE J. Quantum Electron. **21**, 1303 (1985).

8. G. P. Agrawal, "Mode-partition noise and intensity correlation in a two-mode semiconductor laser," Phys. Rev. A **37**, 2488 (1988).

9. S. Inoue, H. Ohzu, S. Machida, and Y. Yamamoto, "Quantum correlation between longitudinal-mode intensities in a multimode squeezed semiconductor laser," Phys. Rev. A **46**, 2757 (1992).

10. H. Wang, M. J. Freeman, and D. G. Steel, "Squeezed light from injection-locked quantum well lasers," Phys. Rev. Lett. **71**, 3951 (1993).

11. J. Kitching, A. Yariv, and Y. Shevy, "Room temperature generation of amplitude squeezed light from a semiconductor laser with weak optical feedback," Phys. Rev. Lett. **74**, 3372 (1995).

12. F. Marin, A. Bramati, E. Giacobino, T.-C. Zhang, J.-Ph. Poizat, J.-F. Roch, and P. Grangier, "Squeezing and intermode correlations in laser diodes," Phys. Rev. Lett. **75**, 4606 (1995).

13. S. Inoue and Y. Yamamoto, "Longitudinal mode partition noise in a semiconductor laser based interferometer," Opt. Lett. **22**, 328 (1997).

14. Y. Yamamoto, S. Saito, and T. Mukai, "AM and FM quantum noise ion semiconductor lasers. Part II: Comparison of theoretical and experimental results for AlGaAs lasers," IEEE J. Quantum Electron. **19**, 47 (1983).

15. T.-C. Zhang, J.-Ph. Poizat, P. Grelu, J.-F. Roch, P. Grangier, F. Marin, A. Bramati, V. Jost, M. D. Levenson, and E. Giacobino, "Quantum noise of free-running and externally-stabilized laser diodes," Quantum Semiclassic. Opt. **7**, 601 (1995).

16. M. Homar, S. Balle, and M. San Miguel, "Mode competition in a Fabry–Perot semiconductor laser: travelling wave model with asymmetric dynamical gain," Opt. Commun. **131**, 380 (1996).

17. H. P. Yuen and V. W. S. Chan, "Noise in homodyne and heterodyne detection," Opt. Lett. **8**, 177 (1983).

18. A. L. Schawlow and C. H. Townes, "Infrared and optical masers," Phys. Rev. **112**, 1940 (1958).

19. C. H. Henry, "Theory of the linewidth of semiconductor lasers," IEEE J. Quantum Electron. **18**, 259 (1982).

20. M. A. Newkirk and K. J. Vahala, "Amplitude-phase decorrelation: a method for reducing intensity noise in semiconductor lasers," IEEE J. Quantum Electron. **QE-27**, 13 (1991).

21. A. Karlsson and G. Björk, "Use of quantum-noise correlation for noise reduction in semiconductor lasers," Phys. Rev. A **44**, 7669 (1991).

22. C. B. Su, J. Schlafer, and R. B. Lauer, "Explanation of low-frequency relative intensity noise in semiconductor lasers," Appl. Phys. Lett. **57**, 849 (1990).